Simplified Design Method for Litz Wire

Charles R. Sullivan
Thayer School of Engineering at Dartmouth
Hanover, NH, USA
Email: charles.r.sullivan@dartmouth.edu

Richard Y. Zhang
Dept. Elec. Eng. & Comp. Sci., M.I.T.
Cambridge, MA, USA
Email: ryz@mit.edu

***Abstract*—A simplified approach to choosing number and diameter of strands in litz wire is presented. Compared to previous analyses, the method is easier to use. The parameters needed are only the skin depth at the frequency of operation, the number of turns, the breadth of the core window, and a constant from a table provided in the paper. In addition, guidance is provided on litz wire construction—how many strands or sub-bundles to combine at each twisting operation. The maximum number of strands to combine in the first twisting operation is given by a simple formula requiring only the skin depth and strand diameter. Different constructions are compared experimentally.**

I. Introduction

Litz wire has become an essential tool for power electronics, enabling low-resistance high-current conductors at frequencies up to hundreds of kHz. But applying litz wire effectively is not easy. Simple approaches, such as tables of recommended strand diameter by frequency, can backfire, in some cases leading to higher resistance than a simple solid-wire or foil winding, and almost always leading to higher cost and loss than could be achieved with more careful design. However, the literature on more sophisticated analysis and design approaches can be intimidating, with recommended approaches including Bessel functions [1]–[5], combinations of Bessel functions [6] or iterative application of them [7]; as well as complex permeability models [8], [9], among others [10]. Even the relatively simple approach in [11] requires a formula with ten terms raised to various powers. Furthermore, these methods generally only help with choosing the number of strands, and offer little guidance on the details of construction—the number of strands that should be combined at each step of twisting. (For example, 120-strand litz wire could be constructed as 12×10, as 8×5×3, or as 3×5×8.)

This paper offers a simplified approach to choosing the number and diameter of litz-wire strands, and shows that it is equivalent to the more complex approaches in other work. The approach can easily be implemented with a spreadsheet but is also simple enough for hand calculations. Its simplicity makes it useful for practicing engineers, and also makes it easier for practitioners and researchers to gain insight into the design problem and loss phenomena. The paper also offers a simple rule-based approach to choosing the construction once the number and diameter of strands has been chosen.

II. Instructions for Using the Method

For fast reference, this section provides step-by-step instructions for the basic method, as applied to a layer-wound transformer, and the following section extends the method to gapped inductors. The theoretical basis and justification for the method are discussed later, in Section IV. Fig. 1 outlines the complete process.

A. Choosing number and diameter of strands

The four steps in the process to choose the number and diameter of strands correspond to the first four boxes in Fig. 1.

1) Compute skin depth: The skin depth is given as

$$\delta = \sqrt{\frac{\rho}{\pi f \mu_0}} \tag{1}$$

where ρ is the resistivity of the conductor ($1.72 \times 10^{-8}\Omega$·m for copper at room temperature, or $2\times10^{-8}\Omega$·m at 60°C), f is the frequency of a sinusoidal current in the winding, and μ_0 is the permeability of free space ($4 \times 10^{-7}\pi$ H/m). Using MKS units for all variables in this equation results in skin depth in meters. For non-sinusoidal currents and combinations of dc and ac current, the same formula for skin depth (1) can be used if the frequency is replaced by the effective frequency introduced in [11] and reviewed in Appendix A.

2) Winding parameters: The winding parameters needed for the calculation, b and N_s, are illustrated in Fig. 2 for some common winding geometries. b is the breath of the winding, across the face where one winding faces another, and N_s is the number of turns in the section of the winding in question. In simple windings without interleaving, N_s is simply the number of turns in the winding being designed ($N_s = N$). With interleaving, it is the number of turns counting from a zero field surface to the face between the primary and secondary. The zero-field surface is either against a high-permeability core, or at the center of a winding in a symmetrical interleaved design.

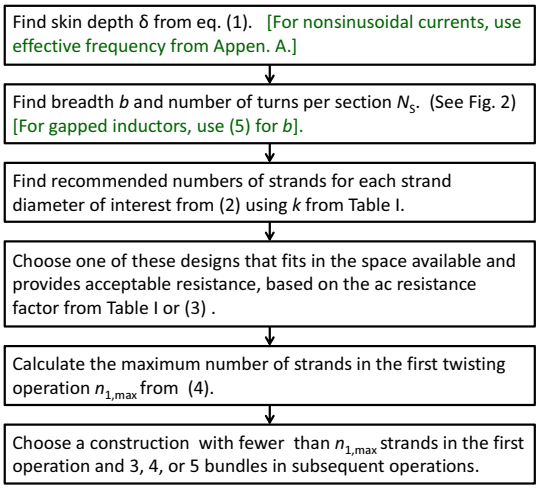

Fig. 1. Flowchart of the litz wire design method. Optional extensions for non-sinusoidal waveforms and for gapped inductors are in [ ], in green.

TABLE I
PARAMETERS FOR ECONOMICAL LITZ-WIRE DESIGNS. k IS USED IN (2).

Strand AWG size	32	33	34	35	36	37	38	39	40	41	42	43	44	45	46	47	48
Strand diameter (mm)	0.202	0.180	0.160	0.143	0.127	0.113	0.101	0.090	0.080	0.071	0.063	0.056	0.050	0.045	0.040	0.035	0.032
Economical F_R	1.06	1.07	1.09	1.11	1.13	1.15	1.18	1.22	1.25	1.30	1.35	1.41	1.47	1.54	1.60	1.64	1.68
k (mm^{-3})	130	203	318	496	771	1.2k	1.8k	2.8k	4.4k	6.7k	10k	16k	24k	36k	54k	79k	115k

3) Recommended number of strands: The next step is to calculate a recommended number of strands for each of the strand diameters being considered, using

$$n_e = k\frac{\delta^2 b}{N_s} \tag{2}$$

where k is a constant for each strand diameter, given in Table I. In the table, k is given in units of mm^{-3}, so b and δ should also be in units of mm, such that a unitless value of n_e results.

The recommended values of n_e given by (2) should be taken as general indications not precise prescriptions. Values of n as much as 25% above or below n_e can still be good choices.

4) Final strand diameter and number selection: From (2) a range of good design options for different strand diameters is produced. To select one of these, first check whether the designs given by (2) fit in the window space available. A rough first approximation for this calculation is to assume that the total area of actual copper, NnA_s, where N is the number of turns, n is the number of strands, and A_s is the cross sectional area of a single strand, must be less than 25 to 30% of the window area available for that winding. If the number of strands recommended does not fit in the window, one may consider using the largest number that fits instead, but if this requires reducing the number of strands by more than about 25%, using one of the designs that does fit will have almost as good performance at significantly lower cost.

When the number of strands is chosen as n_e, the ac resistance factor is as given in Table I. From this information and a simple calculation of dc resistance, it is straightforward to compile a table of the ac resistance of the economical and effective designs for each of the strand diameters considered, providing a range of possible tradeoffs between loss and cost. Given a loss (and thus ac resistance) spec, one can choose the lowest cost design meeting that spec from the table.

If the number of strands to be used deviates from the values given by (2), either because space constraints or availability of the wire, the ac resistance factor for any number of strands can be calculated by

$$F_R = \frac{R_{ac}}{R_{dc}} = 1 + \frac{(\pi n N_s)^2 d_s^6}{192 \cdot \delta^4 b^2} \tag{3}$$

where n is the number of strands actually used and d_s is the strand diameter. Note that ensuring the right units are used in this formula is simply a matter of making sure all of the lengths (d_s, δ, and b) are all in the same units (e.g., all in mm). The accuracy and scope of applicability of this formula is discussed in Section IV.

Winding designers often follow a rule regarding "circular mils per amp" or "amps per square mm." If this is a concern, see Appendix B for further guidance.

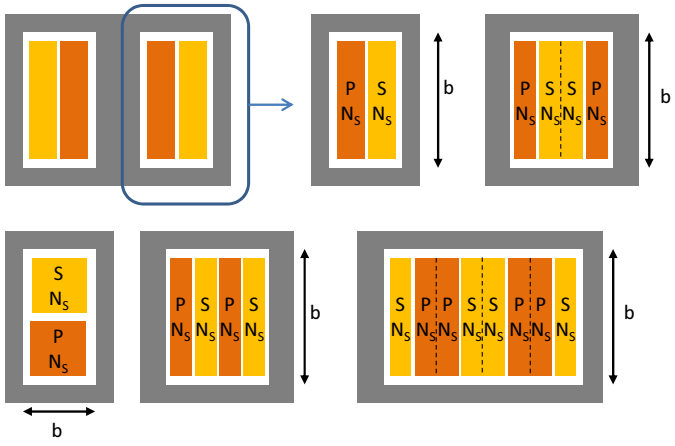

Fig. 2. Examples of how the winding breadth b and the number of turns per section are defined for some common winding geometries. Each section shown has a number of turns N_s; depending on whether the different sections of a given winding (primary P or secondary S) are in parallel or series, the total number of turns N for that winding may be equal to N_s or equal to product of N_s and the number of sections. Note that N_s may be different for the primary and secondary windings.

B. Choosing construction

If a large number of strands is simply twisted together, rather than constructed with multiple levels of twisting (sometimes called "true litz" construction), there can be a bundle-level skin-effect problem: the high-frequency current will preferentially flow in the surface strands, while the inner strands are underutilized [11]. The construction needed to avoid this problem can be determined as follows.

The approximate maximum recommended number of single strands to be twisted together in the first step is

$$n_{1,max} = 4\frac{\delta^2}{d_s^2} \tag{4}$$

where δ is the skin depth for a solid conductor given by (1) and d_s is the diameter of an individual strand.

If the total number of strands, n is less than $n_{1,max}$, then all the strands can be simply twisted in one operation without problems from bundle-level skin effect. If $n > n_{1,max}$, then multiple twisting operations may improve performance. The first twisting step should combine $n_{1,max}$ or fewer strands. Subsequent operations should only combine 3, 4, or 5 bundles from preceding operations.

For example, with $d_s = \delta/4$, $n_{1,max} = 64$. For $n \leq 64$, a single simple twisting operation is all that is needed. For larger numbers of strands, multiple operations are needed. The first operation can combine up to 64 strands. The next operation can combine up to 5 of the 64-strand bundles to make litz wire with up to 320 total strands. Then up to 5 of those 320 strand

(5×64) bundles can be combined to make litz wire with up to 1600 strands (5×5×64). Other numbers of strands can be created or approximated by using any number up to 64 in the first step, and 3, 4, or 5 in the subsequent steps.

The value of $n_{1,max}$ given by (4) is conservative. Adhering to this limits guarantees avoiding problems, as discussed further in conjunction with the experimental results in Section VI.

III. Gapped Inductors

Gapped inductors have a strong field near the gap, which can induce large losses in any conductors placed in that region. Spacing the winding away from the gap is a well established technique to address this problem. The optimal positioning of the wire away from the gap, and rigorous optimization of litz wire in this case is developed in [12]–[15], for which software is available for download or to run online at [16]. Rather than trying to improve on that work, which provides true optimized designs, the objective here is to provide a much simpler analysis that can be used to choose a reasonable litz stranding with less effort.

With a winding configuration such as that shown in Fig. 3, the same equation for a good number of strands to choose, (2), can be used, but with b replaced by an effective value,

$$b_{\text{eff}} = \pi \left(0.693 \cdot r_1 + 0.307 \cdot r_2^{0.91} \cdot r_1^{0.09}\right) \tag{5}$$

where r_1 and r_2 are the inner and outer radii of the winding region as shown in Fig. 3.

As can be seen from (5), the effective value of b is a weak function of r_2 in Fig. 3. As a result, the outer edge of the winding region does not need to be a semicircle as shown in Fig. 5. r_2 can be replaced with an approximate average distance from the gap to the outer edge of the winding and used in (5). This average distance can be roughly estimated or can be more systematically calculated based on making the winding area of the annular region between r_1 and r_2 in Fig. 3 equal to that of the real winding shape.

Note that in inductors that carry ac and dc current, another good option is to use a semicircular litz-wire winding in parallel with another winding that only carries dc current (or low-frequency current) [10], [17]. In such a case, the design method presented here can be used to design the litz winding stranding.

For an ungapped inductor on a low permeability core, a rough approximation is the use the perimeter of the winding for b.

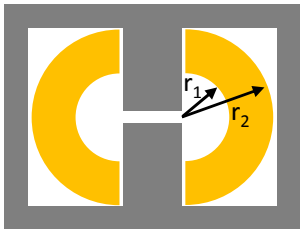

Fig. 3. Winding spaced away from an inductor air gap by a radius r_1.

IV. Basis of the Method

A. Loss calculation

The basis of the loss calculation used here is a direct calculation of the eddy currents and resulting loss induced in a cylinder subjected to a uniform transverse magnetic field. One approach to that calculation is to derive the exact analytical solution for a single isolated cylinder immersed in a uniform field extending infinitely far away from the cylinder. This results in a Bessel function solution [1]–[5]. This is an exact solution for a single wire with nothing near it, but is only an approximation when wires are closer together [7], [9], [10], [18], and is usually no better than the seemingly less sophisticated Dowell method [19] when wires are tightly packed together as in a winding [18], [20]. Fortunately, the discrepancy between actual behavior and the Bessel-function solution is only at high frequencies, where $d_s > \delta$, outside the range of good design practice. Thus, for design, the Bessel function approach is adequate.

However, in the useful design range where $d_s \leq \delta$, and the Bessel function formulation is accurate, it is also overkill. The formula can be greatly simplified by taking only the first terms of a series expansion of the Bessel function solution. Alternatively, an *identical* formula can be derived directly from a simple physical analysis of the eddy currents induced in a cylinder with a uniform transverse field, by assuming that the field penetrates the cylinder uniformly without being significantly reduced by the self-shielding effect of the eddy currents. Because the skin effect is the manifestation of such self-shielding behavior, the assumption of a field uniformly penetrating the cylinder is valid for $d_s < \delta$. Thus, such a simple analysis is valid over the same range of d_s/δ in which the Bessel function approach works well, which is also the range of interest for design. Since the Bessel function approach is more complex and offers no advantage in the range of interest, we use the simplified formulation.[1]

The simplified formulation for the eddy-current loss in a cylinder for $d_s \leq \delta$ is given in [21] and is also derived in more detail in [22] as

$$P(t) = \frac{\pi \ell d_c^4}{64\rho} \left(\frac{dB}{dt}\right)^2 \tag{6}$$

For a sinusoidal waveform, the time average value of the squared derivative of $B(t)$ is $\omega^2 \hat{B}^2/2$, where ω is the radian frequency and $\hat{B}$ is the peak amplitude of the field, so the time-average loss becomes

$$P = \frac{\pi \ell d_c^4 \omega^2 \hat{B}^2}{128\rho} \tag{7}$$

as it is presented in [21]. These formulations are valid for any field shape. For a winding configuration that results in a field strength that linearly increases as the winding builds up and is constant across the breadth (a 1-D field), this results in an ac resistance factor [11]

$$F_R = 1 + \frac{\pi^2 \mu_0^2 N^2 n^2 \omega^2 d_c^6}{768 \rho^2 b^2} \tag{8}$$

[1] An additional reason to avoid the Bessel function formulation is that many researchers have been fooled into thinking that it is an exact wideband solution for a winding, when it is in fact only exact for widely spaced wires, the opposite extreme compared to tightly packed wires in winding.

Here, we suggest a slight reformulation of (8) which makes it incrementally, but perhaps significantly, simpler and easier to use. From (1),

$$\frac{2}{\delta^2} = \frac{\omega\mu_0}{\rho}. \tag{9}$$

Substituting results in

$$F_R = \frac{R_{ac}}{R_{dc}} = 1 + \frac{(\pi n N)^2 d_s^6}{192 \cdot \delta^4 b^2} \tag{10}$$

In addition to being simpler, (10) has the advantage that is it easy to see how the dimensions work: the numerator and denominator both have dimensions of length to the sixth power. Moreover, because (3) is based on direct physical analysis of a cylindrical conductor, it avoid errors associated with approximating round conductors as square or rectangular. As discussed above, it is valid when $d_s < \delta$ and for a 1-D field geometry. The implications of these assumptions and alternatives for other situations are discussed in Section V.

B. Choosing number and diameter of strands

Finding a way to calculate the ac resistance factor F_R is only the first step towards choosing a design. Even with a target value for F_R chosen, there are many combinations of number and diameter of strands that could be used to achieve the same value of F_R. One design approach would be to hold the number of strands fixed and find the optimum diameter; another would be to hold the diameter fixed and find the optimum number of strands. Both of these are analyzed in [11]. An approach that is better linked to real-world applications is to hold the loss fixed and find the minimum cost design. This problem was addressed in a complex way in [23], but the results can be condensed to a simple table of the most economically efficient value of F_R for a given strand diameter (Table I). By plugging values of F_R from the table into (3), and solving for the effective and economical recommended number of strands n_e, we obtain

$$n_e = \frac{\delta^2 b \sqrt{192(F_R - 1)}}{\pi N d_s^3} \tag{11}$$

To simplify the application of this formula, we can pre-compute

$$k = \frac{\sqrt{192(F_R - 1)}}{\pi d_s^3} \tag{12}$$

and tabulate the k values for use in the very simple formula

$$n_e = k\frac{\delta^2 b}{N} \tag{13}$$

Because the values of F_R from [23] are based on cost data that is now more than a decade old, new cost data was compared to the model, and the parameters for the cost curve-fit function in [23] were adjusted slightly to $k_1 = 6 \times 10^{-26}$ m^{-6} and $k_2 = 2.7 \times 10^{-9}$ m^{-2}. The values in Table I are based on these new parameters. The cost data used was incomplete and users may wish to adapt the parameters and recalculate the table based on pricing offered by their suppliers, using (4) and (5) in [23] and (12) above.

Values of n near those provided by (13) will provide reasonable ac resistance factors (as shown in Table I), and will give a good economical tradeoff between cost of litz wire and ac resistance. Calculating the number of strands for different diameters (and thus different values of k) gives a range of options from low-cost designs with a small number of low-cost large-diameter strands to high-performance designs with a much larger number of much finer strands.

C. Construction

Given a choice for the number and diameter of strands, the sequence of twisting operations still must be selected. The goal is to construct the wire such that the current flowing in each strand will be approximately equal. The primary effects that could lead to unequal current between strands would be proximity effect and skin effect at the bundle level. Bundle-level proximity effect is current circulating between different strands, and bundle-level skin effect is current flowing in the strands near the surface of a bundle (or sub-bundle) while strands running down the center are underutilized [11]. Bundle-level proximity effect is combatted simply by twisting, and the design criterion that results is just that the pitch of twisting must be small compared to the overall length of wire, or to the length of wire exposed to a given field strength.

Bundle-level skin effect, on the other hand, is not impacted by simple twisting, and must be combatted by construction techniques that transpose strands between different radial positions in the bundle over the length. This is primarily done by using multi-level construction: first twisting together n_1 strands of magnet wire, and then twisting together n_2 of those sub-bundles, followed optionally by additional stages of twisting. One approach to avoiding skin effect to to make sure that, at each stage, no more than five strands or sub-bundles are twisted together. A group of five or fewer has no strand in the center, whereas a group of seven has six around the outside and one in the center. A group of six doesn't work as neatly as a group of seven, but is likely to fall into a similar configuration with one in the center.

For example, to make a 100-strand bundle, one could start by twisting five magnet wires together, then twist five of those lowest-level sub-bundles together, and finally twist four of those larger sub-bundles together to get a bundle of 100 strands with no skin effect beyond the strand-level skin effect that is made negligible by using strands much smaller than a skin depth. This would be designated as 4/5/5 if the twisting at each level was in the same direction ("bunching operations"), or as 4×5×5 if the twisting alternated directions at each level ("cabling operations").

By only combining strands or sub-bundles in groups of 3, 4, or 5, one can completely avoid bundle-level skin effect for any of the bundling levels. However, this approach results in a large number of operations which increases the cost, and also increases the dc resistance, as each operation introduces a few percent increase in length to the actual strand path. Fortunately, such an extreme approach is rarely necessary. In a typical scenario, bundle-level skin effect is not an issue for the first steps of the construction. For example, a typical design might use strand diameters of one quarter of a skin depth. A construction that started with twisting together seven such strands would not have any problems with skin effect, because the overall diameter of that first sub-bundle would only be 3/4

of a skin depth. Skin effect does not become significant until the diameter is at least two skin depths.

The procedure in Section II-B for choosing a construction is based on first, calculating the maximum number of strands for which the bundle diameter is less than two skin depths, and using that as $n_{1,max}$, the maximum number of strands for the first operation. This avoids bundle-level skin effect at the first level. Each subsequent operation is constrained to use 3, 4, or 5 sub-bundles, and thus avoids any further bundle-level skin effect.

The calculation of the number of strands for which the bundle diameter is less than two skin depths is complicated by the fact that we need to know the skin depth not in a solid conductor, but in a medium comprising copper strands separated by thin insulation and airspace. As a rough approximation, we adopt the straightforward approach taken in [6] of using the average conductivity for this composite medium. Under this assumption, the effective skin depth for the bundle is

$$\delta_{\text{eff}} = \frac{\delta}{\sqrt{F_{p,litz}}} \tag{14}$$

where $F_{p,litz}$ is the litz packing factor, defined as the ratio of the total copper cross-sectional area in the bundle ($n\pi d_s^2/4$) to the area of the overall bundle ($\pi d_b^2/4$). The ratio of the bundle diameter to effective skin depth is

$$\frac{d_b}{\delta_{\text{eff}}} = \frac{d_b}{\delta}\sqrt{F_{p,litz}} = \frac{d_b}{\delta}\sqrt{\frac{n\pi d_s^2/4}{\pi d_b^2/4}} = \frac{d_s}{\delta\sqrt{n}} \tag{15}$$

Setting this ratio equal to 2 for the maximum allowable number of strands in the first twisting operation ($n_{1,max}$) results in

$$n_{1,max} = 4\frac{\delta^2}{d_s^2} \tag{16}$$

where δ is the skin depth for a solid conductor given by (1) and d_s is the diameter of an individual strand.

D. Gapped Inductors

The effect of the gap fringing field on litz wire near it can be described by the average value of B^2 in the region of the winding [22]. To make an approximate calculation of that field, we assume the winding is spaced away from the gap a distance r_1, and that its shape is as shown in Fig. 3, or that that shape is a reasonable approximation. The assumption that the winding is spaced away from the gap limits the applicability of this analysis, but spacing the winding way from the gap is usually a good idea.

For this analysis, we analyzed the geometry in Fig. 3 in rectangular coordinates rather than considering the curvature of the wire around the center post, both to simplify the mathematical analysis and to simplify the application of the method by reducing the number of input variables. In this case, the field lines are semicircles around the gap, with field strength

$$B(r) = \frac{\mu_0 I}{\pi r} \tag{17}$$

in the region between the gap and the winding. Inside the winding, this is reduced by a factor equal to the fraction of the winding area outside of the radius at which the field is being evaluated, such that

$$B(r) = \frac{\mu_0 I}{\pi r}\frac{(r_2^2 - r^2)}{(r_2^2 - r_1^2)} \tag{18}$$

Averaging B^2 over the winding area, and comparing to the spatial average of the squared field in the one dimensional case

$$\langle B^2 \rangle = \frac{\mu_0^2 I^2}{3b^2} \tag{19}$$

we can find a value of b_{eff} that gives the same value of $\langle B^2 \rangle$ as the field in (18) when used in (19):

$$b_{\text{eff}} = \frac{\pi(r_2^2 - r_1^2)^{1.5}}{r_2^2\sqrt{\ln\frac{r_2}{r_1} + \frac{r_1^2}{r_2^2} - \frac{r_1^4}{4r_2^4} - 0.75}} \tag{20}$$

Because (20) is overly complicated for the theme of this paper, we found a curve fit for it (5) with parameters optimized to minimize the maximum percentage error at any point in the region of r_2/r_1 up to 100. The fit has less than 1% error over this range.

In Section III it is stated that (5) can provide adequate accuracy even when the outer boundary of the winding is not a semicircle. To test this, we ran a 2-D finite-element simulation of a PQ35/35 core with a 1 mm centerleg gap and a winding that fills the winding window except for a 5 mm radius semicircular region near the gap. An equivalent of r_2 was calculated as 11 mm based on matching the actual winding area to the area of a semicircular region between $r_1 = 5$ mm and r_2. The calculated value of $b_{\text{eff}} = 20.77$ mm results in an estimate of $\langle B^2 \rangle$ 14% higher than the simulated value. This is adequate accuracy for an approximate analysis, considering the fact that the winding actual winding region is a significantly different shape (the window is 25 mm $\times$ 8.8 mm).

V. Discussion and Alternatives

The basic analysis provided here is accurate for 1-D overall field geometries and for frequencies where $d_s \leq \delta$. It is more accurate than Dowel's approximation, because it is not based on approximating round wires with "equivalent" foil, but is instead based on a direct calculation of loss in the actual round wire shape. However, it starts to overestimate loss for higher frequencies, beyond where $d_s \approx 2\delta$. This is not a problem for design work, because good designs won't use combinations of strand diameters and frequencies that get into that region.

The primary limitation is the restriction to a 1-D field as with transformer geometries like those shown in Fig. 2, or to gapped inductors using the formulation developed in Section IV-D and presented in Section III. For arbitrary field shapes, and for situations in which different windings have different waveform shapes, the approach in [24] provides a rigorous optimization of litz wire cost and loss for arbitrary geometries and waveforms, albeit one requiring more complex software.

As discussed above, the restriction of strand diameter smaller than a skin depth is not a problem for design work, as good designs of litz wire will use strands smaller than a skin depth, often by a factor of 4 or more. Occasionally it is useful to estimate ac resistance for a much higher frequency.

For example, if a waveform has high-frequency harmonics, the optimization might provide a design for which $d_s < \delta$ for the fundamental, but not for the harmonics. Correcting the loss estimate for the harmonics is rarely essential, but is sometimes of interest. In these cases, it is shown in [7], [9], [10], [18], [20] that neither the Dowell approach nor the Bessel function approach yields an accurate solution, with the exception of the iterative Bessel function approach described in [7]. It is shown in [20] that a curve-fit approach can offer higher accuracy; a similar, simpler, lower-accuracy formulation is provided in [10]. These formulations can be applied directly to estimate loss from a calculated 1-D field or a 2- or 3-D field from simulation or calculation, or can be reformulated as a complex permeability for use in finite element simulations [8], [9]. A computationally streamlined approach for finding a wideband model that gives accurate loss estimation based on these approaches is provided in [25], where a 2-D magnetostatic field analysis is combined with loss models to yield a frequency-dependent resistance matrix that can be used to calculate loss for any set of current waveforms in a multi-winding component.

Note that the restriction to a 1-D field geometry only refers to the overall field shape, not to the local phenomena as the wires interact with the field and incur loss. The actual 2-D circular shape of the wires is used in the loss calculation.

The assumption of a linearly increasing field through the winding is an approximation, but for litz wire, it is actually a better approximation than assuming a stepwise layer-by-layer increase in field, as the field gradually increases as one moves up through the strands of a litz-wire layer. Simulations and measurements consistently confirm the validity of this approach.

One aspect of wire construction that is not addressed here is the choice of the twisting pitch. In general, a wide range of pitches can work well, and the choice of pitch may be left to the litz wire manufacturer based primarily on practical considerations. Numerical simulations of the effects of pitch reported in [26] provide more insight into the effects of pitch and may lead to more specific guidance. A possible concern in this regard is turns that are close to an air-gap. Such a turn might be subject to a strong field just through a fraction of one twist of the wire. The twisting of litz wire works to reduce proximity effect when voltage induced by the flux through one half twist is canceled by the same flux going through the next half twist, linked in the opposite sense [26]. If the flux at the next half twist is much lower because it is not as close to the gap, this principle is undermined.

VI. Experimental Measurements

The ac winding resistance formulation upon which the strand number and diameter design method is based (8) is already well validated, but very little work has been published examining the effect of litz construction on bundle-level skin effect, so we concentrate on experiments to validate the construction recommendations in Section II-B, and in particular (4).

One valuable data source is [6] which includes measurements of ac resistance without external proximity effect, and furthermore compares two constructions with the same total number of strands (245) and with the same strand diameter (0.1 mm). This makes it possible to see the effect of bundle construction. The two constructions measured were 7×35/(0.1 mm) and 4×(61 or 62)/(0.1 mm). Of these, only the second follows the construction guidelines in Section II-B; the first violates these by combining more than 5 bundles in the second operation. And, confirming this guideline, the 7×35/(0.1 mm) construction exhibits worse performance when the two are compared in [6].

The number of strands in the lowest-level bundle, n_1, is 61 or 62 for the 4×(61 or 62)/(0.1 mm) construction measured in [6]. From (4), this would be permissible for a frequency of 29 kHz or lower. The data in [6] confirms that this wire has no deviation from ideal behavior below 29 kHz; but it also shows very little deviation from ideal behavior at higher frequencies, which may indicate that the configuration of the 61 or 62 strand bundle includes some transposition. Thus, [6] provides one data point for which following the guidelines in Section II-B would avoid any problems, but it falls short of clearly demonstrating the importance of specifically limiting the number of strands in the first level of construction to the value in (4).

To more fully examine the effect of construction on bundle-level skin effect, we constructed three litz wires, each with 125 strands of AWG 34 (0.16 mm) magnet wire. One was simply twisted (125/(0.16 mm)), one used a cabling operation to combine 5 bundles, each with 25 strands (5×25/(0.16 mm)), and the final construction attempted to avoid all bundle-level skin effect by combine five strands or bundles at each step ($5 \times 5 \times 5$/(0.16 mm)). We constructed these by hand using basic ropemaking equipment [27] in order to ensure we knew the exact sequence of operations. The three constructions are shown in Fig. 4.

Measurements of dc resistance for a 2 m length yield 14.307 mΩ ($5 \times 5 \times 5$/(0.16 mm)), 14.35 mΩ (5×25/(0.16 mm)), and 14.46 mΩ (125/(0.16 mm). These are 5 to 6% higher than the theoretical resistance for 125 straight strands of AWG 34 wire in parallel, a result of the increased length from twisting and possibly also imperfect termination

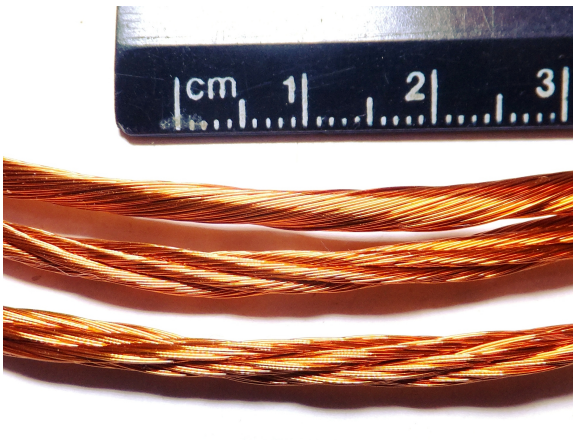

Fig. 4. Three constructions for 125 strands of 0.16 mm diameter magnet wire: Top: simply twisted (125/(0.16 mm)); middle: 5×25/(0.16 mm); bottom: $5 \times 5 \times 5$/(0.16 mm).

or strand breakage, resulting in fewer than 125 strands actually conducting.

Measurements of ac resistance are shown in Fig. 5. The measurements are for the same 2 m lengths, laid out in a serpentine (zig-zag) pattern with approximately 8 cm spacing to minimize proximity effect and inductance. The measurements use an Agilent 4294A impedance analyzer with a Kelvin clip test fixture with short leads (about 10 cm). The results clearly show that the $5 \times 5 \times 5$ construction provides the best performance, that 5×25 provides the second-best performance, and simply twisted 125-strand wire ranks last, consistent with our predictions.

Quantitatively, (4) indicates that $n_1 = 25$ is fine up to 25 kHz. The measured resitance for the 5×25 construction first becomes clearly worse than the $5 \times 5 \times 5$ construction between 30 and 40 kHz, consistent with (4). The 125-strand simply twisted wire is only guaranteed to avoid bundle-level skin effect up to about 5.5 kHz based on (4), but no degradation in performance is distinguishable from noise until above about 25 kHz. In this case, the wire works better than would be expected in the 6 kHz to 25 kHz range.

In summary, the data show that:

- Following the construction guidelines in Section II-B always yielded good results.
- The performance improves as the construction approaches ideal litz, combining no more than 5 strands or bundles in any given operation, but more strands can be safely combined in the first operation if the maximum number given by (4) is not exceeded.
- Of the three constructions evaluated, two worked well to higher frequencies than would be predicted by (4), but one showed performance degradation just above the safe frequency predicted based on (4). Thus, it appears that (4) is a valid worst-case calculation but some bundles work better than it predicts.

The fact that (4) is overly conservative for some samples and not for others can be explained by the fact that simply twisted a bunch comprising a large number of wires can easily result in a complex and somewhat random structure, rather than the ideal of a single strand that goes the full length down the center, followed by successive concentric helical shells. The 125 strands that were simply twisted were first looped on two hooks 3 meters apart, and then one hook was twisted while the other was held fixed. There was no attempt to position the wires in a specific configuration at either end, and the positions of the strands in the bundle could easily be very different at the two ends. The randomization of the strand positions worked reasonably well in this case, and the resulting wire performed well at up to 25 kHz. However, this is not a good way to guarantee good performance, and attempting to better control the production might yield worse results.

To illustrate the behavior that can occur with a more controlled construction, the simulation tool described in [26] was used to simulate the same three constructions, but with the 25 and 125 strand simply twisted bundles having an ideal structure in which all the strands stay at the same radius throughout the length. The results are shown in Fig. 6. These results more clearly confirm (4), with the simply-twisted and 5×25 constructions deviating from the ideal $5 \times 5 \times 5$ construction at the expected 5.5 and 25 kHz frequencies, respectively. The deviations are much more dramatic than those in Fig. 5, consistent with our explanation that the simply twisted bundles include some random radial transposition.

Based on the experimental and simulation results it is recommended to use the procedure in Section II-B to determine a construction that can guarantee consistently achieving good results. Note that in many cases, this will yield a recommendation to use a construction that is considerably simpler than might be required if the strictest guideline (to never combine more than 5 strands) was followed.

VII. Conclusion

Previous literature on litz wire provides complex methods for choosing the number and diameter of strands for litz wire, but does not address the details of construction. This paper presents a simplified approach to choosing the stranding, and provides, for the first time, a straightforward guide to choosing

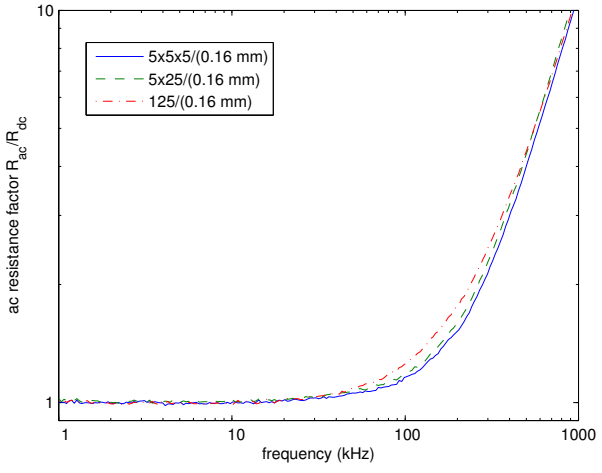

Fig. 5. Measured ac resistance factor of three constructions for 125 strands of 0.16 mm diameter magnet wire. The three types are simply twisted (125/(0.16 mm)); a construction with simple twisting of 25 strands followed by a cabling operation 5×25/(0.16 mm); and "true litz" $5 \times 5 \times 5$/(0.16 mm).

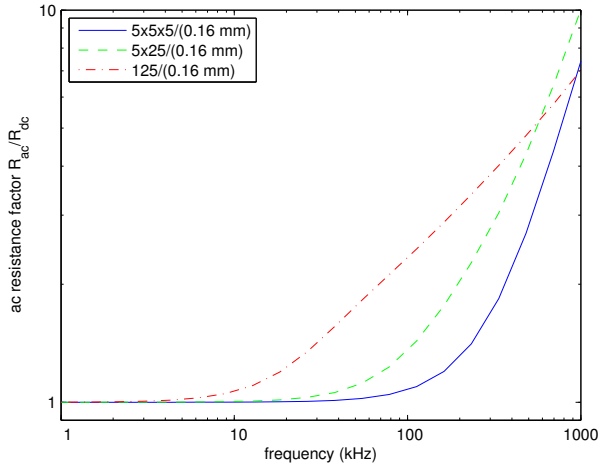

Fig. 6. Numerically simulated ac resistance factor for the same nominal constructions of 125 strand litz wire as in Fig. 5. The simulation method used is described in [26].

the construction. Experiments and numerical simulations are consistent with the construction guidelines provided.

Appendix A
Effective Frequency

Replacing the frequency in (1) with an effective frequency, as explained in detail in the appendix of [11] can be used to apply the optimization method presented here (and similar optimization methods for other types of windings) to non-sinusoidal waveforms, including waveforms with ac and dc components. The effective frequency is defined as

$$f_{\text{eff}} = \frac{\text{rms}\left\{\frac{di(t)}{dt}\right\}}{2\pi I_{\text{rms}}} \tag{21}$$

Note that to account for dc, the rms value used should be inclusive of the dc component, i.e., $I_{\text{rms}} = \sqrt{I_{\text{ac,rms}}^2 + I_{\text{dc}}^2}$. A very helpful reference for rms values and rms values of derivatives is Table II of [28]. Note, however, that the optimum thickness formulas given in that table are only valid for foil windings, not for round wire, because of the different constraints that apply, whereas (21) is more broadly applicable.

Appendix B
Note on Current Density

Traditionally, rules for maximum current density have provided useful guidance for wire selection; these are usually stated in A/mm^2 or "circular mils" per ampere. At dc or low frequency, the power dissipation per unit volume of copper can be calculated from the current density. For example, at 650 circular mils per amp (3.04 A/mm^2), using the resistivity of copper at 60°C, the power dissipation density is 184 mW/cm^3 in the copper, or overall in a winding with a packing factor of 0.5, 92 mW/cm^3. How much temperature rise this results in depends on, among other things, the surface area to volume ratio of the component. Such rules were established for 50/60 Hz components, and then applied without adjustment to high-frequency components for power electronics. The result often worked because loss density was much higher (sometimes by a factor of 3 or more because of proximity effect losses), but the surface area to volume ratio was also much higher for the smaller high-frequency components. However, a well-designed high-frequency winding will not have such severe proximity-effect losses. Thus, one can take advantage of the high surface area to volume ratio and run much higher current densities. When a bobbin is underfilled, this increases the surface area to volume ratio, and allows still higher current densities.

A good design procedure is to establish an allowable total dissipation in an given winding based on a thermal model (e.g., [29]) or test, and then model losses that ensure they stay below that limit. In any case, in comparing two designs with similar surface area, a design with lower winding dissipation is preferred, even if it has higher nominal current density.

References

[1] J. A. Ferreira, "Analytical computation of ac resistance of round and rectangular litz wire windings," *IEE Proceedings-B Electric Power Applications*, vol. 139, no. 1, pp. 21–25, Jan. 1992.

[2] ——, "Improved analytical modeling of conductive losses in magnetic components," *IEEE Trans. on Pow. Electr.*, vol. 9, no. 1, pp. 127–31, Jan. 1994.

[3] J. Acero, P. J. Hernandez, J. M. Burdío, R. Alonso, and L. Barragdan, "Simple resistance calculation in litz-wire planar windings for induction cooking appliances," *IEEE Trans. on Magnetics*, vol. 41, no. 4, pp. 1280–1288, 2005.

[4] J. Acero, R. Alonso, J. M. Burdio, L. A. Barragan, and D. Puyal, "Frequency-dependent resistance in litz-wire planar windings for domestic induction heating appliances," *IEEE Trans. on Pow. Electr.*, vol. 21, no. 4, pp. 856–866, 2006.

[5] C. Carretero, J. Acero, and R. Alonso, "Tm-te decomposition of power losses in multi-stranded litz-wires used in electronic devices," *Progress In Electromagnetics Research*, vol. 123, pp. 83–103, 2012.

[6] H. Rossmanith, M. Doebroenti, M. Albach, and D. Exner, "Measurement and characterization of high frequency losses in nonideal litz wires," *IEEE Trans. on Pow. Electr.*, vol. 26, no. 11, pp. 3386–3394, 2011.

[7] M. Albach, "Two-dimensional calculation of winding losses in transformers," in *IEEE Pow. Electr. Spec. Conf*, vol. 3. IEEE, 2000, pp. 1639–1644.

[8] Xi Nan and C. R. Sullivan, "An equivalent complex permeability model for litz-wire windings," in *Fortieth IEEE Industry Applications Society Annual Meeting*, 2005, pp. 2229–2235.

[9] D. C. Meeker, "An improved continuum skin and proximity effect model for hexagonally packed wires," *Journal of Computational and Applied Mathematics*, vol. 236, no. 18, pp. 4635–4644, 2012.

[10] A. van den Bossche and V. Valchev, *Inductors and Transformers for Power Electronics*. Taylor and Francis Group, 2005.

[11] C. R. Sullivan, "Optimal choice for number of strands in a litz-wire transformer winding," *IEEE Trans. on Pow. Electr.*, vol. 14, no. 2, pp. 283–291, 1999.

[12] J. Hu and C. R. Sullivan, "Optimization of shapes for round-wire high-frequency gapped-inductor windings," in *Proceedings of the 1998 IEEE Industry Applications Society Annual Meeting*, 1998, pp. 900–906.

[13] ——, "Analytical method for generalization of numerically optimized inductor winding shapes," in *IEEE Pow. Electr. Spec. Conf.*, 1999.

[14] C. R. Sullivan, J. McCurdy, and R. Jensen, "Analysis of minimum cost in shape-optimized litz-wire inductor windings," in *IEEE Pow. Electr. Spec. Conf*, 2001.

[15] R. Jensen and C. R. Sullivan, "Optimal core dimensional ratios for minimizing winding loss in high-frequency gapped-inductor windings," in *IEEE Applied Power Electronics Conference*, 2003, pp. 1164 –1169.

[16] "Dartmouth power electronics and magnetic components group web site," http://power.engineering.dartmouth.edu.

[17] C. Schaef and C. Sullivan, "Inductor design for low loss with complex waveforms," in *IEEE Applied Power Electronics Conference*, 2012.

[18] Xi Nan and C. R. Sullivan, "An improved calculation of proximity-effect loss in high-frequency windings of round conductors," in *IEEE Pow. Electr. Spec. Conf*, 2003.

[19] P. Dowell, "Effects of eddy currents in transformer windings," *Proceedings of the IEE*, vol. 113, no. 8, pp. 1387–1394, Aug. 1966.

[20] Xi Nan and C. R. Sullivan, "Simplified high-accuracy calculation of eddy-current loss in round-wire windings," in *IEEE Pow. Electr. Spec. Conf*, 2004.

[21] E. C. Snelling, *Soft Ferrites, Properties and Applications*, 2nd ed. Butterworths, 1988.

[22] C. R. Sullivan, "Computationally efficient winding loss calculation with multiple windings, arbitrary waveforms, and two- or three-dimensional field geometry," *IEEE Trans. on Pow. Electr.*, vol. 16, no. 1, pp. 142–50, 2001.

[23] ——, "Cost-constrained selection of strand wire and number in a litz-wire transformer winding," *IEEE Trans. on Pow. Electr.*, vol. 16, no. 2, pp. 281–288, Mar. 2001.

[24] J. D. Pollock, T. Abdallah, and C. R. Sullivan, "Easy-to-use CAD tools for litz-wire winding optimization," in *IEEE Applied Power Electronics Conference*, 2003.

[25] D. R. Zimmanck and C. Sullivan, "Efficient calculation of winding loss resistance matrices for magnetic components," in *IEEE Workshop on Control and Modeling for Power Electronics (COMPEL)*, 2010.

[26] R. Y. Zhang, C. R. Sullivan, J. K. White, and J. G. Kassakian, "Realistic litz wire characterization using fast numerical simulations," in *IEEE Applied Power Electronics Conference (APEC)*, 2014.

[27] Lacis, "Leonardo rope machine." [Online]. Available: http://www.lacis.com/catalog

[28] W. Hurley, E. Gath, and J. Breslin, "Optimizing the ac resistance of multilayer transformer windings with arbitrary current waveforms," *IEEE Trans. on Pow. Electr.*, vol. 15, no. 2, pp. 369–76, Mar. 2000.

[29] W. G. Odendaal and J. A. Ferreira, "A thermal model for high-frequency magnetic components," *IEEE Trans. on Ind. Appl.*, vol. 35, no. 4, pp. 924–931, 1999.